Role of heavy-meson exchange in pion production near threshold

C. J. Horowitz*
Department of Physics and Nuclear Theory Center, Indiana University, Bloomington, Indiana 47405

H. O. Meyer
Department of Physics and Cyclotron Facility, Indiana University, Bloomington, Indiana 47405

David K. Griegel†
Department of Physics and Nuclear Theory Center, Indiana University, Bloomington, Indiana 47405
(Received 7 April 1993)

Recent calculations of s-wave pion production have severely underestimated the accurately known $pp \to pp\pi^0$ total cross section near threshold. In these calculations, only the single-nucleon axial-charge operator is considered. We have calculated, in addition to the one-body term, the two-body contributions to this reaction that arise from the exchange of mesons. We find that the inclusion of the scalar σ-meson exchange current (and lesser contributions from other mesons) increases the cross section by about a factor of 5 and leads to excellent agreement with the data. The results are sensitive neither to changes in the distorting potential that generates the NN wave functions nor to different choices for the meson-nucleon form factors.

PACS number(s): 11.40.Ha, 13.60.Le, 13.75.Cs

I. INTRODUCTION

Recently, a precise measurement of the total cross section for pion production in the reaction $pp \to pp\pi^0$ was carried out using the electron-cooled stored beam of the Indiana University Cyclotron Facility (IUCF) Cooler with an internal gas target [1]. The novel technology made it possible to extend the measurements to within a few MeV of threshold. Over most of the covered energy range, contributions from higher partial waves are negligible, and the cross section is thus due to a single partial wave ($^3P_0 \to {}^1S_0 + s$-wave pion). That this is the case can be deduced from the energy dependence of the cross section and the angular distribution of the outgoing protons [1].

As we will discuss below, s-wave pion production is sensitive to the axial charge of the two-nucleon system. A number of calculations using the single-nucleon axial-charge operator [2–4,1] have been carried out with various choices for the NN distorting potentials. Quite surprisingly, such calculations all underestimate the data by approximately a factor of five. This discrepancy is even more serious since there is little ambiguity in the calculations, because only a single partial wave is involved, and the NN wave functions and the (free) operator are both well known.

The discrepancy could be explained by an enhancement of the axial charge in the NN system, which could come from a relativistic effect. There exist many relativistic calculations for nuclear systems; for example, relativistic impulse-approximation calculations [5,6] accurately reproduce elastic proton-nucleus scattering data. Relativistic models characteristically feature large Lorentz scalar and vector potentials [7]. The strong scalar potential enhances the lower component of the Dirac wave function of the nucleon; this change enhances the axial charge [8] (see Sec. IV). Several authors have examined the consequences of this relativistic effect on β decay or muon capture rates in $A = 16$ nuclei [9] and nuclei near $A = 208$ [10].

In nonrelativistic models, relativistic effects can be incorporated formally via meson-exchange currents (MEC's). In this view the relativistic effect would be represented by a MEC involving a scalar σ meson. Note that σ exchange also provides a phenomenological model for the intermediate-range attraction in the NN interaction and is responsible for part of the spin-orbit potential. Many authors have examined MEC contributions to the axial-charge operator in nuclei, and found that the largest contribution is due to $\pi\rho$ exchange [11], which enhances axial-charge matrix elements by about 60%. The next largest MEC is believed to be the relativistic σ exchange, contributing another 40% to the axial charge. Together these contributions could account for the approximately 100% enhancement seen in axial-charge matrix elements for a variety of β decays [11]. However, the size of the MEC contribution that one would derive from experiment depends on assumptions about complicated wave functions and short-range NN correlations.

Because of isospin considerations, the $\pi\rho$ current (proportional to the dot product of $\vec{\tau}_1 \times \vec{\tau}_2$ and the pion field) cannot contribute to $pp \to pp\pi^0$. However, other MEC's may well be important. In this case, pion production in the pp system would provide a unique laboratory for

*Electronic address: charlie@venus.iucf.indiana.edu
†Present address: Department of Physics, University of Maryland, College Park, MD 20742.

testing MEC models for a number of reasons. First, the initial proton must decelerate in order to produce a pion. The resulting large momentum mismatch can best be mediated by meson exchange. Heavy mesons are favored; indeed, the initial relative momentum near threshold of about 1.9 fm^{-1} is comparable to the mass of the σ meson. Thus the process is very sensitive to two-body contributions. Second, contributions from intermediate states with a nucleon and a spin-$\frac{3}{2}$ Δ are expected to be small, since such a system cannot be formed in a relative s state because of angular momentum considerations. Furthermore, the Δ cannot decay into a spin-$\frac{1}{2}$ nucleon and an s-wave pion. (Reference [4] provides estimates of Δ contributions.) Third, pion-rescattering effects are believed to be small, because the scattering length for pion-nucleon s-wave scattering in the required isospin combination is small, as will be discussed in Sec. II. Finally, the wave functions in this case are simple and can be calculated reliably.

Lee and Riska [12] have recently suggested that the inclusion of MEC's could explain the magnitude of the observed $pp \to pp\pi^0$ total cross section. They calculate MEC's by assuming a simple operator form for the NN potential. This allows the calculation of MEC's for phenomenological potentials, but depends on model assumptions. In this paper, we perform a similar calculation; however, we use an explicit one-boson-exchange model for the NN interaction as well as for the calculation of meson-exchange contributions. We also include the Coulomb interaction, which is quite important near threshold. Furthermore, we examine the sensitivity of the calculated cross section to many of the model ingredients.

In Sec. II we outline the formalism for the calculation and discuss the input parameters and some computational details. In Sec. III we collect and discuss the results for a variety of one-body and two-body contributions and for different NN interactions. Section IV lists the conclusions from our work.

II. FORMALISM AND DETAILS OF THE CALCULATION

In this section we present the formalism used to calculate the total $pp \to pp\pi^0$ cross section for s-wave pion production. The calculation is carried out in coordinate space, because this allows for a simple treatment of the Coulomb interaction between the two protons. The first three subsections are devoted to the matrix elements that correspond to the production mechanisms illustrated by the diagrams in Fig. 1, namely, (a) the one-body term and the two-body terms that arise either from (b) pion rescattering or (c) the exchange of heavier mesons. In Sec. II D we collect a number of calculational details and give the expression for the total cross section.

A. One-body matrix element

The one-body term [Fig. 1(a)] can be viewed as a nucleon radiating a pion in the distorting potential of the other nucleon. The interaction between the two nucleons is needed in order to conserve energy and momentum.

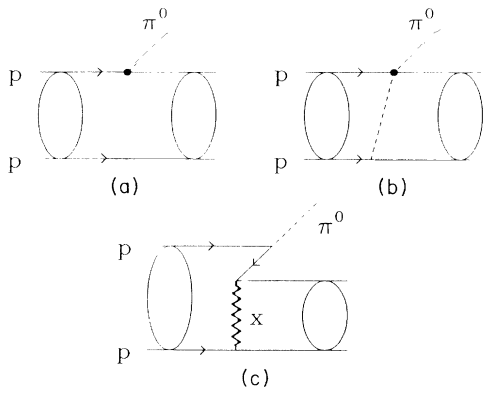

FIG. 1. Contributions to the reaction $pp \to pp\pi^0$. Shown are (a) the one-body term, (b) the two-body term that arises from pion rescattering, and (c) the two-body term that arises from the exchange of heavier mesons (x).

We start with the pseudovector interaction Lagrangian between the pion field $\vec{\phi}$ and the nucleon field ψ [13],

$$\mathcal{L}_{\rm int} = -\frac{f_{\pi NN}}{m_\pi}\overline{\psi}\gamma_5\gamma^\mu\vec{\tau}\psi\cdot\partial_\mu\vec{\phi}\,, \tag{1}$$

where $f_{\pi NN}$ is the pion coupling constant and m_π is the pion mass. A *pseudoscalar* Lagrangian (proportional to $\overline{\psi}\gamma_5\vec{\tau}\psi\cdot\vec{\phi}$), instead of Eq. (1), would yield the same one-body contribution; however, *pseudovector* coupling is favored for reasons that are discussed in Sec. II C.

The field operators in Eq. (1) involve sums over operators that create or destroy particles of a given momentum [14]. The term

$$\mathcal{M}_{fi} \propto \overline{U}_{s'}(p')(\gamma_5\gamma_0 q_0 - \gamma_5\boldsymbol{\gamma}\cdot\mathbf{q})U_s(p) \tag{2}$$

is responsible for the emission of a neutral pion of momentum q by a proton of momentum p. Here U is a proton Dirac spinor, and $p' = p - q$ is the final proton momentum. The second term in Eq. (2) has the nonrelativistic limit $\gamma_5\boldsymbol{\gamma} \to -\boldsymbol{\sigma}$, where $\boldsymbol{\sigma}$ stands for the conventional 2×2 Pauli spin matrices. This term, which represents the familiar nonrelativistic $\boldsymbol{\sigma}\cdot\mathbf{q}$ pion coupling, is *odd* under spatial reflection of the pion, $\mathbf{q} \to -\mathbf{q}$. It is thus responsible for the production of pions with odd angular momentum (p wave or higher). Since, near threshold, the production of p-wave pions is suppressed by the angular momentum barrier, we are interested here only in the first term in Eq. (2), which, being *even* under spatial reflection, can describe the production of s-wave pions. The existence of this term is a consequence of Lorentz invariance, which requires both a timelike and spacelike part to be present in the original pseudovector ($\gamma_5\gamma_\mu q^\mu$) coupling.

Alternatively, coupling to an s-wave pion can also be generated from a nonrelativistic $\boldsymbol{\sigma}\cdot\mathbf{q}$ coupling term by invoking Galilean invariance. Clearly, the coupling should involve a dot product between $\boldsymbol{\sigma}$ and the momentum of

the pion *relative* to the nucleon, rather than just the momentum $\mathbf{q}$ of the pion. However, since m_π is so much smaller than the mass M of the nucleon, the relative momentum differs from $\mathbf{q}$ by only a small recoil term involving the nucleon momentum $\mathbf{p}$. Thus we expect a $\boldsymbol{\sigma}\cdot\mathbf{p}$ coupling term from the nucleon recoil, which can produce s-wave pions, that is smaller than the $\boldsymbol{\sigma}\cdot\mathbf{q}$ term by a factor of m_π/M. The nonrelativistic limit of the first term in Eq. (2),

$$\overline{U}_{s'}(p')\gamma_5\gamma_0 q_0 U_s(p) \simeq -\frac{m_\pi \chi^\dagger_{s'}\boldsymbol{\sigma}\cdot(\mathbf{p}+\mathbf{p}')\chi_s}{2M} , \quad (3)$$

is precisely this recoil contribution, where, near threshold, we take $q_0 \simeq m_\pi$.

It is straightforward to evaluate the contribution of the one-body term in Fig. 1(a) for the partial wave $^3P_0 \to {}^1S_0$. The result for the corresponding matrix element is [2]

$$J_1 = -\frac{m_\pi^2}{pp'}\int_0^\infty dr\, j_0\left(\frac{q'r}{2}\right) u_0(r)\left(\frac{d}{dr}+\frac{1}{r}\right) u_1(r) . \quad (4)$$

Here u_0 and u_1 are distorted coordinate-space wave functions for the $^1S_0$ and $^3P_0$ channels, p and p' are the initial and final relative momenta of the two nucleons, and q' is the pion momentum in the final pp center-of-mass frame. The distorted waves are normalized such that

$$u_L(r) \to \sin\left(pr - \frac{\pi L}{2} + \delta_L\right) , \quad (5)$$

as $r \to \infty$, where δ_L is the corresponding phase shift. An analogous prescription applies when, asymptotically, Coulomb wave functions are used.

When the IUCF Cooler data [1] became available, it was immediately clear that the one-body cross section, calculated with J_1 alone, does *not* reproduce the data, underestimating the experiment by about a factor of five [1]. This discrepancy is so much larger than any uncertainty in the calculation of J_1 that the conclusion is unavoidable that there must be significant *additional* contributions to s-wave pion production, over and above the one-body term discussed so far.

B. Pion rescattering

An obvious mechanism for pion production that involves both nucleons is the so-called pion-rescattering diagram shown in Fig. 1(b). We note that in Eq. (4) the wave function for a free pion is used, while the two nucleons appear as distorted waves. One might argue that the pion-rescattering diagram represents the first correction that arises from the distortion of the *pion*. The matrix element J_π for the rescattering contribution, derived from a simple phenomenological pion-nucleon s-wave interaction, is given in Ref. [2] as

$$J_\pi = \frac{\lambda_1 m_\pi}{pp'}\int_0^\infty dr\, j_0\left(\frac{q'r}{2}\right) u_0(r) \times\left[f(r)\left(\frac{d}{dr}+\frac{1}{r}\right)+\frac{M}{m_\pi}\left(2+\frac{m_\pi}{2M}\right)\frac{df}{dr}\right] u_1(r) . \quad (6)$$

The radial function f is defined as $f(r) \equiv e^{-\mu r}/r$, where $\mu = \sqrt{\frac{3}{4}}m_\pi$.

The pion-rescattering matrix element in Eq. (6) scales with the parameter λ_1. This parameter is obtained from the appropriate isospin average of the pion-nucleon s-wave scattering lengths $a_{1/2}$ and $a_{3/2}$, corresponding to isospin $\frac{1}{2}$ and $\frac{3}{2}$:

$$\lambda_1 = -\frac{m_\pi}{6}(a_{1/2}+2a_{3/2}) . \quad (7)$$

Koltun and Reitan [2], as well as other authors more recently [3,4], use the older value of

$$\lambda_1^{\rm KR} = 0.005 , \quad (8)$$

while Lee and Riska [12], making use of the computer code SAID [15], favor the value

$$\lambda_1^{\rm LR} = -0.0023 . \quad (9)$$

In both cases, pion-nucleon phase shifts have been extrapolated down to threshold from energies where scattering data are available. The two values differ because of new data added during the past 25 years and also because of different constraints in the extrapolation procedure. On the other hand, there exists experimental information that is more directly related to the scattering lengths. For instance, from the branching ratios of the decay of pionic hydrogen [16], one obtains $a_{1/2} - a_{3/2} = 0.263 \pm 0.005 m_\pi^{-1}$; from the measured $1s$ width of pionic hydrogen [17], one obtains $2a_{1/2}+a_{3/2} = 0.258 \pm 0.012 m_\pi^{-1}$. Combining the two results yields

$$\lambda_1 = 0.001 \pm 0.002 . \quad (10)$$

We conclude that, so far, there is no experimental evidence that λ_1 differs from zero or, consequently, that on-shell pion rescattering contributes to $pp \to pp\pi^0$. Nevertheless, we will explore the sensitivity of the calculated cross section to a possible nonzero value of λ_1 in Sec. III.

Alternatively, one can calculate pion-rescattering contributions using a phenomenological chirally symmetric Lagrangian. For example, Adam *et al.* [18] calculate an axial MEC by considering fully retarded one-pion exchange and three other diagrams. For our process, the retarded pion exchange gives zero [their Eq. (2.12a)], while the other diagrams are all proportional to $\vec{\tau}_1 \times \vec{\tau}_2$ and, hence, make no contribution to $pp \to pp\pi^0$. Thus this approach also predicts very small pion rescattering.

Whether an off-shell treatment of the pion-nucleon rescattering vertex results in a much larger contribution remains to be seen. It may be possible to investigate this by using a chiral Lagrangian and working to higher order in derivatives. Alternatively, one could use a full three-

body model of the πNN system. For the remainder of the paper we will restrict ourselves to the on-shell matrix element, Eq. (6).

C. Exchange of heavy mesons

In this subsection we discuss the exchange of mesons heavier than the pion. Clearly, meson exchange, where the intermediate state is a positive-energy nucleon, is already contained in the distorted waves used for evaluating the one-body term in Fig. 1(a), as is explicitly manifest in the construction of the Bonn potential. However, a virtual, negative-energy state as shown in Fig. 1(c) is *not* contained in the nonrelativistic wave functions. Therefore, this contribution must be explicitly added to the pion-production operator as a two-body correction.

The matrix element for Fig. 1(c) is calculated using elementary Feynman rules [14]. Let us first consider scalar-isoscalar σ-meson exchange (other heavy mesons will be discussed below). Neglecting distortions for a moment, this matrix element is given schematically by

$$\mathcal{M}_{fi} \propto \overline{U}'_2 U_2 \left(\frac{g_\sigma^2}{m_\sigma^2 - k_\mu^2}\right) \overline{U}'_1 \left[\left(\frac{V\overline{V}}{2M}\right) \gamma_5\gamma_0 q_0 + \gamma_5\gamma_0 q_0 \left(\frac{V\overline{V}}{2M}\right)\right] U_1 \ , \tag{11}$$

where k_μ is the momentum of the exchanged σ meson, and U_1 and U'_1 (U_2 and U'_2) are the initial and final Dirac spinors for the first (second) proton. In Eq. (11) we have only included the antinucleon contribution $V\overline{V}/2M$ for the Feynman propagator of the intermediate nucleon, taking the nonrelativistic limit $k_0 + E_k \simeq 2M$ for the energy denominator (there is an implicit sum over the spin indices of V and $\overline{V}$). Also, we have only kept the $\gamma_5\gamma_0 q_0$ part of the pion-nucleon vertex, since we are interested in s-wave pions. The two terms in Eq. (11) correspond to the two possible orderings for the emission of the σ meson and the emission of the pion.

It is a simple matter to take the nonrelativistic limit of Eq. (11) by expanding to lowest order in $1/M$. This yields

$$\mathcal{M}_{fi} \propto -\frac{1}{M}\left(\frac{g_\sigma^2}{m_\sigma^2 + \mathbf{k}^2}\right) \frac{m_\pi \chi_1'^\dagger \boldsymbol{\sigma}\cdot(\mathbf{p}+\mathbf{p}')\chi_1}{2M} \ . \tag{12}$$

Here $\mathbf{k}$ is the momentum transferred by the σ meson, and $\mathbf{p}$ and $\mathbf{p}'$ are the initial and final momenta of the first nucleon. Equation (12) then represents an additional two-body contribution to the effective nonrelativistic operator that describes pion production. This term can be directly compared to the one-body term in Eq. (3), which has a very similar form, except that the two-body term contains an additional factor of $1/M$ and a factor $g_\sigma^2/(\mathbf{k}^2 + m_\sigma^2)$ from the σ-meson propagator. It is important to realize that the one-body and σ-meson exchange contributions [Eqs. (3) and (12)] have the same sign. Thus the two-body contribution will interfere constructively with the one-body term.

We now express Eq. (12) in coordinate space, by taking the Fourier transform, and then calculate the matrix element with nonrelativistic distorted waves. The momenta $\mathbf{p}$ and $\mathbf{p}'$ become gradient operators that act on the distorted waves. These give rise to a factor $(d/dr + 1/r)$ as in Eq. (4). The meson propagator is transformed to a radial function $f_\sigma(r)$ that contains the mass m_σ and the coupling constant g_σ. This function has the general form

$$f_x(r) = \frac{g_x^2}{4\pi}\frac{e^{-m_x r}}{r} \ , \tag{13}$$

where $x = \{\sigma, \delta, \omega, \rho\}$. Finally, the contribution to Fig. 1(c) from the exchange of the σ meson ($x = \sigma$) becomes

$$J_\sigma = -\frac{m_\pi^2}{pp'}\int_0^\infty dr\, j_0\left(\frac{q'r}{2}\right) u_0(r)\frac{f_\sigma(r)}{M} \times \left(\frac{d}{dr} + \frac{1}{r}\right) u_1(r) \ . \tag{14}$$

Equation (14) is identical to Eq. (4) except for the extra factor of $f_\sigma(r)/M$. In contrast to the situation with J_1 [Eq. (4)], the inclusion of the pion wave function $j_0(q'r/2)$ is not crucial in this case because of the short range of $f_\sigma(r)$.

As mentioned later, we obtain the NN distorted waves from the coordinate-space version of the Bonn one-boson-exchange potential. The boson masses and coupling constants needed to construct this potential have been fit to NN scattering data and are listed in Table A.3 of Ref. [19]. For consistency, we use the *same* parameters in calculating the exchange contributions discussed here. We also adopt the technique described in Eq. (A.28) of Ref. [19] to include monopole form factors at all meson-nucleon vertices, according to the prescription

$$g_x \to g_x \frac{\Lambda_x^2 - m_x^2}{\Lambda_x^2 - k_\mu^2} \ , \tag{15}$$

where k_μ is the transferred momentum and Λ_x is the cutoff mass (also listed in Table A.3 of Ref. [19]).

In the following, we also consider the contributions to the diagram in Fig. 1(c) from the exchange of mesons other than the σ meson, again using the corresponding parameters from the Bonn potential. We will find later that these contributions are small compared to J_σ.

Let us begin with the scalar-isovector δ meson. Its contribution J_δ has the form of Eq. (14) with the appropriate mass m_δ and coupling g_δ used in Eq. (13):

$$J_\delta = -\frac{m_\pi^2}{pp'}\int_0^\infty dr\, j_0\left(\frac{q'r}{2}\right) u_0(r)\frac{f_\delta(r)}{M}\left(\frac{d}{dr} + \frac{1}{r}\right) u_1(r) \ . \tag{16}$$

For $pp \to pp\pi^0$ the isospin factors are the same for the exchange of either an isoscalar or an isovector meson. The contribution from the exchange of a vector-isoscalar ω meson can be calculated in a similar fashion. It contributes a term

$$J_\omega = -\frac{m_\pi^2}{pp'}\int_0^\infty dr\, j_0\left(\frac{q'r}{2}\right) u_0(r) \times\left[\frac{f_\omega(r)}{M}\left(\frac{d}{dr}+\frac{1}{r}\right)+\left(\frac{1}{2M}\right)\frac{df_\omega}{dr}\right] u_1(r)\ . \tag{17}$$

The contribution from the exchange of a vector-isovector ρ meson has the form of Eq. (17), with the exception of a nonvanishing tensor coupling:

$$J_\rho = -\frac{m_\pi^2}{pp'}\int_0^\infty dr\, j_0\left(\frac{q'r}{2}\right) u_0(r) \times\left[\frac{f_\rho(r)}{M}\left(\frac{d}{dr}+\frac{1}{r}\right)+\left(\frac{1+C_\rho}{2M}\right)\frac{df_\rho}{dr}\right] u_1(r)\ . \tag{18}$$

Here $C_\rho = 6.1$ is the ratio of the tensor to vector coupling for the ρ meson [19]. Note that Eq. (18) describes only the ρ-meson contribution to the diagram of Fig. 1(c). In principle, there are other contributions of the ρ meson to the axial charge that arise from a $\pi\rho$ current [11]. However, the $\pi\rho$ current has an isospin factor proportional to the dot product between the pion field and $\vec{\tau}_1 \times \vec{\tau}_2$ and, therefore, does not contribute to the reaction $pp \to pp\pi^0$. Again, we modify Eqs. (16)–(18) to include form factors following Eq. (A.28) of Ref. [19].

In principle, contributions from the exchange of pseudoscalar π and η mesons to the diagram in Fig. 1(c) are possible. These contributions would be large if pseudoscalar coupling (γ_5) were used in Eq. (1). However, there are several arguments in favor of pseudovector coupling ($\gamma_5\gamma_\mu q^\mu$) [20,21]. For example, pseudoscalar coupling (alone, without any sigma-pi coupling) implies an unrealistically large s-wave pion-nucleon scattering length. In contrast, pseudovector coupling yields zero (to lowest order) for the scattering lengths, in agreement with experiment and consistent with the (experimentally supported) value of $\lambda_1 = 0$ for the pion-rescattering term (see Sec. II B). After adopting pseudovector coupling, MEC contributions from π and η mesons vanish to lowest order in $1/M$.

D. Calculational details and total cross section

The first step in the calculation is the evaluation of the NN distorted waves u_1 and u_0 in the entrance and exit channels. To this aim we make use of the coordinate-space version of the Bonn one-boson-exchange potential, as described in Appendix A.3 of Ref. [19]. The form-factor correction is applied according to the prescription in Eq. (A.28) of Ref. [19], and the Darwin term (proportional to ∇^2) is included following Ref. [22]. Masses, coupling constants, and cutoff masses are listed in Table A.3 of Ref. [19] for all contributing mesons. In that table, two sets of parameters are listed: Bonn potential A (BPA) and Bonn potential B (BPB). They differ in the contribution of the η meson and in the values of the cutoff parameters. In order to test the sensitivity of the calculation to the distorting potential and to connect to earlier results [1], we have obtained distorted waves also from the Reid soft-core (RSC) and Reid hard-core (RHC) potentials [23].

The next step is the evaluation of the one-body contribution J_1 [Eq. (4)]. This depends only on the NN wave functions and the pion-nucleon coupling constant. For the latter, we adopt the value $f^2_{\pi NN}/4\pi = 0.075$, which is consistent with the Nijmegen phase-shift analysis [24,25]. In order to compute the very long-ranged integral in Eq. (4), we integrate conventionally from 0 to some $r_{\max}$ and then rotate the contour into the complex plane as explained in Ref. [26]. This changes an integrand that is oscillating like $(\sin r)/r$ into one that is exponentially damped. For calculations without the Coulomb interaction, we choose $r_{\max}$ to be about 7 fm. When the Coulomb interaction is included, $r_{\max}$ is increased to 100 fm in order to be able to use the simplest asymptotic form [27] for Coulomb wave functions in the complex plane. Our results are insensitive to the exact choice of $r_{\max}$. Since the initial state has a relatively large momentum ($p \simeq 1.9$ fm^{-1}), we expect that Coulomb effects in the entrance channel are small, even at threshold. Thus, in our calculation, the Coulomb interaction only affects the $^1S_0$ final state.

The next step, in principle, is determining the pion-rescattering contribution J_π, as in Eq. (6). However, since the rescattering parameter λ_1 seems to be consistent with zero, this step will be omitted except when we investigate the sensitivity of the results to a possible deviation of λ_1 from zero.

Finally, heavy-meson exchange contributions for σ, δ, ω, and ρ mesons are calculated using Eqs. (14) and (16)–(18). These depend on meson coupling constants, masses, and form-factor cutoff masses. For these parameters we use the same values that define the distorting potentials BPA and BPB, discussed above. For this reason, our calculations with BPA and BPB distortions are *self-consistent.* Note that the calculation does not contain any parameters that are adjusted to pion-production data.

The matrix element $J_{\rm tot}$ for the reaction $pp \to pp\pi^0$ is then composed of contributions from the one-body term J_1, from pion rescattering J_π (in principle), and from heavy-meson exchange currents $J_{\rm MEC}$:

$$J_{\rm tot} = J_1 + J_\pi + J_{\rm MEC}\ . \tag{19}$$

As described in Ref. [2], the total cross section is obtained as a phase-space integral over the square of the matrix element,

$$\sigma_{\rm tot} = \frac{4f^2_{\pi NN}}{\pi\beta M m_\pi^5}\int_0^{q'_{\max}} dq'\, q'^2 p' |J_{\rm tot}|^2\ , \tag{20}$$

where β is the laboratory velocity of the projectile, q' is the pion momentum in the final pp center-of-mass system, and p' is the relative momentum of the final protons.

III. DISCUSSION OF RESULTS AND SENSITIVITY TO INGREDIENTS

A. Contributions to the matrix element

We now examine the relative importance of the various contributions to the matrix element $J_{\rm tot}$ [see Eq. (19)]. To this aim, we evaluate $J_{\rm tot}$ for the typical values of $p = 1.9$ fm^{-1}, $p' = 0.2$ fm^{-1}, and $q' = 0.1$ fm^{-1}. The results are listed in Table I, which shows that the σ-meson contribution J_σ is about as large as the one-body term J_1. Furthermore, these two contributions are constructive; therefore, the σ-meson contribution will increase the cross section by about a factor of four.

The next important contribution is from the ω meson (35–45% of the J_1 or J_σ contribution). In comparison, all other terms are significantly smaller. In particular, the pion-rescattering term J_π is small even when the large older value of $\lambda_1 = 0.005$ is used, and the isovector δ- and ρ-meson contributions are very small and tend to cancel each other. For the sake of completeness, we include in $J_{\rm MEC}$ the contributions from *all* heavy mesons; however, it is important to keep in mind that the dominant two-body contribution is due to the scalar σ-meson exchange.

This large J_σ contribution [Eq.(14)] can be easily understood in relativistic models. In these models [5,7,21], the nucleon has an effective mass

$$M^* = M - S \tag{21}$$

from a strong scalar field S. This enhances the lower components in the Dirac spinors U. If spinors of mass M^* are used, Eq. (3) becomes

$$\overline{U}_{s'}(p';M^*)\gamma_5\gamma_0 q_0 U_s(p;M^*) \simeq -\frac{m_\pi \chi^{\prime\dagger}_{s'}\boldsymbol{\sigma}\cdot(\mathbf{p}+\mathbf{p}')\chi_s}{2M^*} . \tag{22}$$

Thus a reduction of the nucleon mass *enhances* the s-wave pion coupling. Let us expand $1/M^*$ to lowest order in $1/M$:

$$\frac{1}{M^*} \simeq \frac{1}{M}\left(1+\frac{S}{M}\right) . \tag{23}$$

If one assumes that the scalar field arises from the second nucleon, or $S = f_\sigma(r)$ [see Eq. (13)], then the second term (S/M), when substituted into Eq. (4), immediately yields the σ-meson contribution of Eq. (14). Thus the scalar field of the second nucleon affects the Dirac spinor of the first nucleon in such a way that the modified spinor has a larger coupling to an s-wave pion. This simple argument also shows that J_1 and J_σ should add constructively.

It is nevertheless surprising that the σ contribution is almost as large as the one-body term, especially since J_σ involves an additional factor of $1/M$. This is explained by realizing that it is not J_σ that is large, but J_1 that is anomalously small. Near threshold, the two nucleons approach each other with a relative momentum $p \simeq 1.9$ fm^{-1}, and yet they must almost stop in order to produce a pion. Because it is difficult to mediate such a large momentum mismatch through the distortions of Fig. 1(a), J_1 is relatively small. On the other hand, the σ-meson propagator in Fig. 1(c) provides an efficient means of transferring momentum. As already pointed out, it is interesting that the σ-meson mass (550 MeV, according to Table A.3 of Ref. [19]) is comparable to $p \simeq 1.9$ fm^{-1}.

The interpretation of the σ-meson contribution deserves comment. Clearly the σ is not a sharp resonance. Instead it is a simple phenomenological model for the important intermediate-range attraction in the NN interaction. Assuming that this attraction transforms as a Lorentz scalar provides a natural explanation of the spin dependence of the NN force [5,7]. We expect a more complicated model of the intermediate-range attraction (such as correlated two-pion exchange) to yield a similar J_σ contribution, provided the attraction transforms as a Lorentz scalar.

TABLE I. Contributions to the total matrix element $J_{\rm tot}$ for an initial nucleon momentum of $p = 1.9$ fm^{-1}, a final nucleon momentum of $p' = 0.2$ fm^{-1}, and a pion momentum of $q' = 0.1$ fm^{-1}. The Bonn one-boson-exchange potentials (BPA and BPB) and the Reid potentials (RSC and RHC) are described in the text. The pion-rescattering contribution J_π assumes $\lambda_1 = 0.005$ [see Eq. (8)].

Potential	J_1	J_σ	J_ω	J_π	J_δ	J_ρ
BPA	−0.174	−0.163	−0.062	−0.042	−0.009	0.009
BPB	−0.165	−0.152	−0.063	−0.044	−0.024	0.011
RSC	−0.143	−0.135	−0.050	−0.038	−0.006	0.008
RHC	−0.126	−0.140	−0.048	−0.040	−0.007	0.009

B. Total cross-section results

In Fig. 2 our calculation is compared with the available $pp \to pp\pi^0$ total cross-section data as a function of η, the maximum pion momentum in the overall center-of-mass frame in units of m_π ($\eta \equiv q_{\rm max}/m_\pi$), or, alternatively, the projectile energy T in the laboratory. The IUCF Cooler data [1] are shown as solid dots (note that there is a 6.6% uncertainty in the normalization of the data that is not shown), while data from previous work are marked with crosses [28], squares [29], bars [30], and diamonds [31]. As is well known by now, the one-body term alone (dashed line) greatly underestimates the data. However, when the two-body contributions are included (solid line), the measured cross sections are reproduced to an extent that is truly remarkable in view of the fact that none of the parameters of the model have been adjusted to pion-production data. The dot-dashed line, which has been obtained without the Coulomb interaction, demonstrates that Coulomb repulsion is responsible for a fairly sizable reduction of the cross section near threshold. All calculations shown in Fig. 2 use the BPA distorting potential.

It has been pointed out earlier [1] that the energy dependence of the s-wave cross section follows from phase space and the final-state interaction between the two (charged) protons. This is sufficient to reproduce the

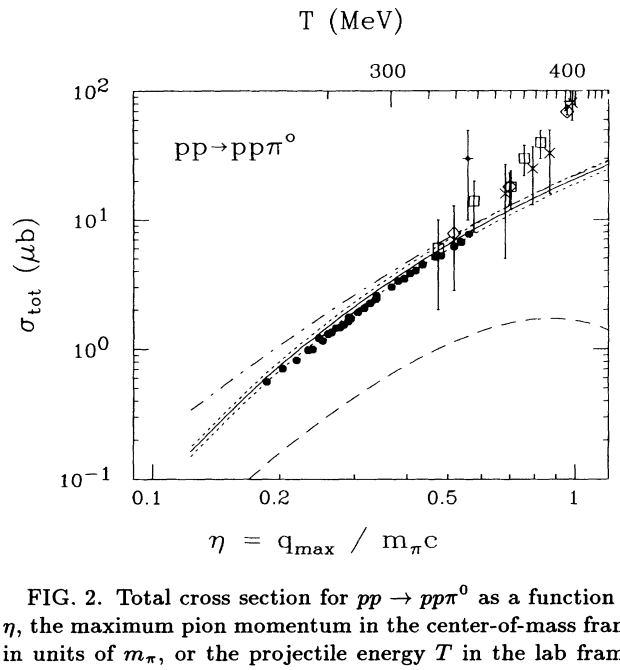

FIG. 2. Total cross section for $pp \to pp\pi^0$ as a function of η, the maximum pion momentum in the center-of-mass frame in units of m_π, or the projectile energy T in the lab frame. The recent IUCF Cooler measurement [1] is shown by solid dots; data from previous work are marked with crosses [28], squares [29], bars [30], and diamonds [31]. The solid line includes heavy-meson exchange and the Coulomb interaction, and the dotted lines describe the error bands for the πN coupling constant $f^2_{\pi NN}/4\pi = 0.075 \pm 0.003$ and the rescattering parameter $\lambda_1 = 0.000 \pm 0.002$ (see text). The dashed line neglects heavy-meson exchange and includes the Coulomb interaction, while the dot-dashed line includes heavy-meson exchange, but neglects the Coulomb interaction. (Note that the Coulomb interaction is included in all other curves in this paper.) All calculations use BPA. The solid curve is the same as in Figs. 4 and 5.

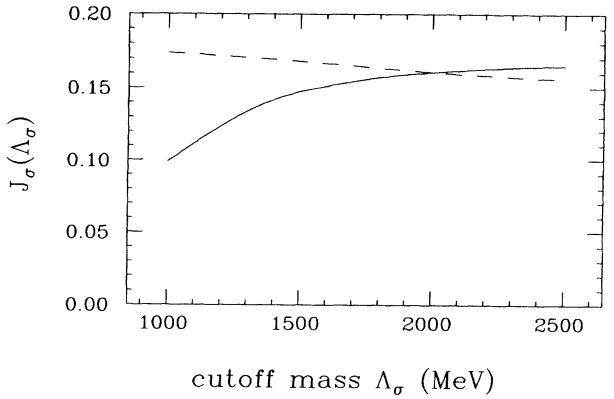

FIG. 3. Dependence of J_σ on the cutoff mass Λ_σ for an initial nucleon momentum of $p = 1.9$ fm^{-1}, a final nucleon momentum of $p' = 0.2$ fm^{-1}, and a pion momentum of $q' = 0.1$ fm^{-1}. The dashed line is obtained by keeping g_σ fixed, while for the solid line $g_\sigma(0)$ was kept constant [see Eq. (24)]. The calculations use BPA, which has the standard cutoff $\Lambda_\sigma = 2$ GeV.

shape of the measured cross section up to $\eta \simeq 0.6$, where higher partial waves (which we are neglecting) start to contribute [1]. Thus it is only the *magnitude* of the cross section near threshold, represented by a single number, that contains nontrivial physics information. Our work shows that heavier meson exchange (mainly of the σ meson), together with the one-body term, is sufficient to explain the observed magnitude of the cross section. In the past, it has been suspected that the role of heavy-meson exchange currents is suppressed by NN correlations and form factors at the meson-nucleon vertices. We find that this is not the case in the NN system: Because of the simplicity of the present reaction, it is possible to explicitly include NN correlations by solving for the full two-body wave function. Even with these correlations included, J_σ remains large.

The dependence of J_σ on the cutoff mass is illustrated in Fig. 3 (using BPA). Note that the form factor in Eq. (15) has a normalization at $k^2_\mu = 0$ that depends strongly on Λ_σ:

$$g_\sigma(0) = g_\sigma \frac{\Lambda^2_\sigma - m^2_\sigma}{\Lambda^2_\sigma} . \tag{24}$$

Indeed, the primary effect of this form factor is to change the value of $g_\sigma(0)$ rather than the momentum dependence of the interaction. It is this coupling near $k^2_\mu = 0$ that plays a dominant role when adjusting the parameters of one-boson-exchange potentials to NN scattering. Therefore it may be more meaningful to compare results with different Λ_σ values at a fixed $g_\sigma(0)$ rather than at a fixed g_σ. Figure 3 shows only a modest decrease of J_σ with decreasing Λ_σ (at fixed g_σ). However, if one keeps $g_\sigma(0)$ fixed rather than g_σ, J_σ actually increases very slightly with decreasing Λ_σ. If two potentials fit phase shifts with different cutoff masses, we expect approximately similar values of $g_\sigma(0)$ (rather than g_σ). If this is the case, the J_σ contribution will be almost independent of Λ_σ.

We now examine the sensitivity to the various distorting potentials that are mentioned in Sec. II D. Figure 4 shows the total cross section, calculated with the Coulomb interaction included and without the pion rescattering term, for the two somewhat different one-boson-exchange potentials BPA (solid line) and BPB (dotted line), and for the RSC (dot-dashed line) and RHC (dashed line) potentials. For the phenomenological Reid potentials there is no way to unambiguously determine the meson-exchange contributions. Therefore, we simply adopt the meson couplings and cutoff masses from BPA for both RSC and RHC. This allows us to study the effects of a change in only the distorted waves u_0 and u_1. The RHC wave functions are identically zero at small distances; in contrast, the RSC wave functions are nonzero, but still small. This enhancement of the wave functions at small r leads to a modest increase in pion production. At small r, the BPA and BPB wave functions are almost identical, but larger still than the RSC wave functions, resulting in a slightly increased cross section. However, some of the difference between the Bonn and Reid results is due to the fact that BPA and BPB generate slightly larger on-shell phase shifts as compared to the Reid po-

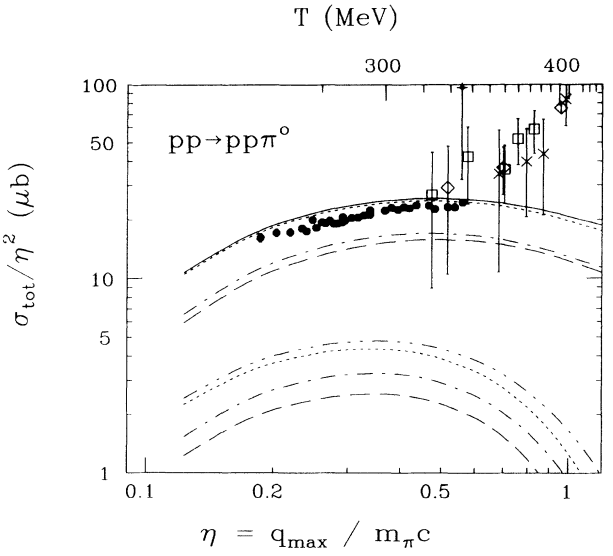

FIG. 4. Sensitivity of the calculated cross section to the distorting potential. Shown is the cross section divided by η^2 as a function of η. The data are the same as in Fig. 2. The curves are for the Bonn potentials A (solid line) and B (dotted lines), and for the Reid soft-core (dot-dashed lines) and Reid hard-core (dashed lines) potentials. The solid curve is the same as in Figs. 2 and 5. The lower four curves are without $J_{\rm MEC}$ (the curves are labeled in the same manner as above, except a dot-dot-dashed curve is used for BPA).

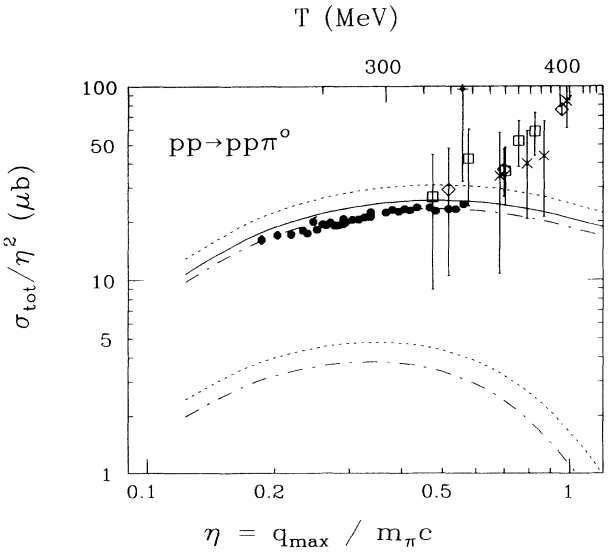

FIG. 5. Sensitivity of the calculated cross section to the rescattering contribution using BPA. Shown is the cross section divided by η^2 as a function of η. The data are the same as in Fig. 2. The curves are for $\lambda_1 = 0.005$ (dotted lines), $\lambda_1 = 0$ (solid line), and $\lambda_1 = -0.0023$ (dot-dashed lines). The solid curve is the same as in Figs. 2 and 4. The lower two curves are without $J_{\rm MEC}$.

tentials. This is because the Bonn potentials are fit to *pn* rather than *pp* data. Nevertheless, the range in cross section for different potentials is still relatively modest. We point out that *all* calculations *without* meson exchange (the lower four curves in Fig. 4) greatly underestimate the data.

Based on the small value for λ_1 in Eq. (10), we do not expect pion rescattering to be important. For completeness sake, we still wish to examine the effect of a possible rescattering contribution. All calculations in Fig. 5 are carried out with BPA and with the Coulomb interaction included. The dotted lines correspond to $\lambda_1 = 0.005$, the dot-dashed lines to $\lambda_1 = -0.0023$, and the solid line is without rescattering. The effect from pion rescattering is relatively small even for the large value $\lambda_1 = 0.005$, and all calculations with only one-body and pion-rescattering contributions (the lower two curves in Fig. 5) fall substantially below the experimental data. Clearly pion rescattering as described by J_π [see Eq. (6)] cannot explain the difference between J_1 and the data. However, one must realize that Eq. (6) is based on a simple on-shell model for pion-nucleon scattering. It is conceivable that the pion-nucleon interaction might be modified due to the fact that the intermediate pion in Fig. 1(b) is off the mass shell. This is a topic that deserves further study.

IV. IMPLICATIONS AND CONCLUSIONS

We have calculated *s*-wave pion production in $pp \to pp\pi^0$ by considering the one-body term, pion rescattering, and two-body meson-exchange processes. We confirm that the one-body term underestimates the data by about a factor of five, and that pion rescattering (in our model) is indeed small. On the other hand, we find a large contribution from the exchange of heavy mesons (in particular, the scalar σ meson) coupling to the negative-energy state of a nucleon, as in Fig. 1(c). This meson-exchange contribution is large enough to explain the discrepancy between one-body production and the data, and, when taken into account with self-consistent distortions, leads to an excellent fit to the data without parameters that are adjusted to pion-production information.

The theoretical description of the $pp \to pp\pi^0$ reaction close to threshold is clean and simple. Only a single partial wave is allowed in either the entrance or exit channels, pion rescattering may be suppressed, and intermediate Δ isobars are expected to be unimportant (in marked contrast to most other reactions involving pions). Furthermore, the simplicity of the system allows a full treatment of NN correlations.

The operator for the production of *s*-wave pions has the same form as the axial-charge operator. Therefore, we conclude that the axial charge in nuclear systems is much larger than what one expects from one-body predictions. This agrees with the conclusions from a number of calculations of first-forbidden β decays in nuclei [11]. However, these nuclear studies are less conclusive because of structure ambiguities. The $pp \to pp\pi^0$ system is free of such ambiguities.

The $pp \to pp\pi^0$ reaction is sensitive to two-body contributions because of the nature of the axial-charge operator and due to a large momentum mismatch that naturally favors the exchange of heavy mesons.

Uncertainties in the meson-nucleon form factors and the two-nucleon wave functions have been examined and are much smaller than the discrepancy between the one-body contribution and the data. Heavy-meson MEC's provide a simple, economical way to account for this discrepancy. However, other alternative explanations may be possible, among them being off-shell pion-rescattering effects.

Using a simple on-shell model we conclude that pion rescattering does not contribute significantly to the cross section. However, it is possible that models of the off-shell πNN vertex could give contributions that are comparable to those from the heavy-meson exchange. Further work should be devoted to a study of full three-body models of the πNN system; however, such calculations are beyond the scope of this paper. Until more is known about the off-shell effects, it seems reasonable to take the on-shell results as a guide and to assume pion rescattering to be small.

If pion rescattering is indeed small, then near-threshold $pp \to pp\pi^0$ data may provide evidence for heavy-meson exchange contributions to the axial current. This is analogous to the electro-disintegration of the deuteron, which provides evidence for electromagnetic MEC's. However, in our system, the MEC's are a very large effect compared to the $\sim 10\%$ contribution to the cross section in the case of the electromagnetic current [32].

To the best of our knowledge, all previous experimental evidence for MEC's has exclusively involved contributions of pionic range. This is significant because of the possibility that heavy-meson contributions are greatly suppressed by NN correlations and meson-nucleon form factors. We have shown that this is *not* the case in the pp system. The importance of heavy-meson exchange currents could be very significant for experiments planned at CEBAF, which, involving higher momentum transfer, are likely to be sensitive to such short-distance effects.

Relativistic nuclear models characteristically feature large Lorentz scalar and vector potentials [7,21]. In these models, the σ meson describes the important intermediate-range attraction in the NN interaction and gives rise to a scalar potential that reduces the effective mass of a nucleon. This reduction in M^* enhances the lower components of Dirac wave functions, and this increases the axial charge. This change in the Dirac wave functions is also what provides the natural description of a large range of nucleon-nucleus scattering data, in particular, spin observables [7]. Our finding that this same effect may explain the observed pion-production cross section also provides an indirect experimental confirmation of this key feature of relativistic models.

The J_σ term in our calculation can be viewed more generally as a term involving some intermediate-range attraction in the NN interaction that transforms like a Lorentz scalar. This contribution does not necessarily have to arise from an elementary narrow σ meson. Instead, it could well be an effective representation of a more complex mechanism. In any case, and whatever the microscopic origin of this Lorentz scalar attraction, its importance in the present calculation may provide evidence for a large relativistic effect in the NN interaction.

Future theoretical work on the $pp \to pp\pi^0$ reaction should be devoted to a study of the off-shell aspects of pion rescattering. Also, the present study should be extended to include the next higher partial waves, as they become important with increasing bombarding energy. This is especially important, since a measurement of the spin-dependent total cross section, which will allow the separation of p-wave pion contributions, is planned at IUCF. This provides the data necessary to search for meson-exchange contributions to Gamow-Teller matrix elements. Since we have found a large and unexpected meson-exchange contribution to the axial charge, we may well speculate about the existence of a similar contribution to Gamow-Teller matrix elements.

This could have important consequences for the $pp \to de^+\nu$ reaction and the solar neutrino problem [33]. This reaction is believed to proceed via a ${}^1S_0 \to {}^3S_1$ Gamow-Teller transition. An enhancement of as little as 15% in the matrix element for $pp \to de^+\nu$ (from an unexpected MEC) would dramatically reduce the disagreement between theory and experiment [34], because, in the standard solar model, the rate of this reaction sensitively affects the central temperature of the sun and thus the high-energy neutrino flux. Of course, present calculations of π and ρ MEC's [35] give only a small contribution. Furthermore, MEC's for this channel are expected to be smaller than the order v/c MEC contributions to the axial charge. However, one may still speculate that some *unsuspected* MEC or other effect could be important. Through very accurate pion-production data it may be possible to gain (indirect) experimental information about the $pp \to de^+\nu$ rate.

ACKNOWLEDGMENTS

C.J.H. and D.K.G. acknowledge support from the U.S. Department of Energy under Grant No. DE-FG02-87ER-40365. H.O.M. acknowledges support from the U.S. National Science Foundation under Grant No. NSF-PHY-9015957.

[1] H. O. Meyer, C. Horowitz, H. Nann, P. V. Pancella, S. F. Pate, R. E. Pollock, B. von Przewoski, T. Rinckel, M. A. Ross, and F. Sperisen, Nucl. Phys. **A539**, 633 (1992).

[2] D. S. Koltun and A. Reitan, Phys. Rev. **141**, 1413 (1966).

[3] G. A. Miller and P. U. Sauer, Phys. Rev. C **44**, R1725 (1991).

[4] J. A. Niskanen, Phys. Lett. B **289**, 227 (1992).

[5] J. R. Shepard, J. A. McNeil, and S. J. Wallace, Phys.

Rev. Lett. **50**, 1443 (1983).
[6] D. P. Murdock and C. J. Horowitz, Phys. Rev. C **35**, 1442 (1987).
[7] B. C. Clark, S. Hama, and R. L. Mercer, in *The Interaction Between Medium Energy Nucleons in Nuclei*, edited by H. O. Meyer (American Institute of Physics, New York, 1983).
[8] J. A. McNeil and J. R. Shepard, Phys. Rev. C **31**, 686 (1985).
[9] G. Do Dang, M. Jaminon, and N. Van Giai, Phys. Lett. **153B**, 17 (1985).
[10] A. O. Gattone, E. D. Izquierdo, and M. Chiapparini, Phys. Rev. C **46**, 788 (1992).
[11] I. S. Towner, Nucl. Phys. **A542**, 631 (1992).
[12] T.-S. H. Lee and D. O. Riska, Phys. Rev. Lett. **70**, 2237 (1993).
[13] S. Weinberg, Phys. Rev. Lett. **18**, 188 (1967).
[14] J. D. Bjorken and S. D. Drell, *Relativistic Quantum Mechanics* (McGraw-Hill, New York, 1964); *Relativistic Quantum Fields* (McGraw-Hill, New York, 1965).
[15] R. A. Arndt, Z. Li, L. D. Roper, R. L. Workman, and J. M. Ford, Phys. Rev. D **43**, 2131 (1991), and the SAID facility mentioned therein.
[16] J. Spuller, D. Berghofer, M. D. Hasinoff, R. MacDonald, D. F. Measday, M. Salomon, T. Suzuki, J.-M. Poutissou, R. Poutissou, and J. K. P. Lee, Phys. Lett. **67B**, 479 (1977).
[17] W. Beer *et al.*, Phys. Lett. B **261**, 16 (1991).
[18] J. Adam Jr., Ch. Hajduk, H. Henning, P. U. Sauer, and E. Truhlik, Nucl. Phys. **A531**, 623 (1991).
[19] R. Machleidt, Adv. Nucl. Phys. **19**, 189 (1989).
[20] C. J. Horowitz and B. D. Serot, Nucl. Phys. **A399**, 529 (1983).
[21] B. D. Serot and J. D. Walecka, Adv. Nucl. Phys. **16**, 1 (1986).
[22] R. Bryan and B. L. Scott, Phys. Rev. **177**, 1435 (1969).
[23] R. V. Reid, Ann. Phys. (N.Y.) **50**, 411 (1968).
[24] J. R. Bergervoet, P. C. van Campen, R. A. M. Klomp, J. L. de Kok, T. A. Rijken, V. G. J. Stoks, and J. J. de Swart, Phys. Rev. C **41**, 1435 (1990).
[25] V. Stoks, R. Timmermans, and J. J. de Swart, Phys. Rev. C **47**, 512 (1993).
[26] C. M. Vincent and H. T. Fortune, Phys. Rev. C **2**, 782 (1970).
[27] *Handbook of Mathematical Functions*, edited by M. Abramowitz and I. A. Stegun (Dover, New York, 1970), p. 540.
[28] R. A. Stallwood, R. B. Sutton, T. H. Fields, J. G. Fox, and J. A. Kane, Phys. Rev. **109**, 1716 (1958).
[29] A. F. Dunaĭtsev and Yu. D. Prokoshkin, Zh. Eksp. Teor. Fiz. **36**, 1656 (1959) [Sov. Phys. JETP **9**, 1179 (1959)].
[30] F. Shimizu, Y. Kubota, H. Koiso, F. Sai, S. Sakamoto, and S. S. Yamamoto, Nucl. Phys. **A386**, 571 (1982).
[31] S. Stanislaus, D. Horváth, D. F. Measday, and A. J. Noble, Phys. Rev. C **41**, R1913 (1990); **44**, 2287 (1991).
[32] D. O. Riska and G. E. Brown, Phys. Lett. **38B**, 193 (1972).
[33] J. N. Bahcall and M. H. Pinsonneault, Rev. Mod. Phys. **64**, 885 (1992).
[34] V. Castellani, S. Degl'Innocenti, and G. Fiorentini, Phys. Lett. B **303**, 68 (1993).
[35] J. Carlson, D. O. Riska, R. Schiavilla, and R. B. Wiringa, Phys. Rev. C **44**, 619 (1991).